

# Effects of hydrostatic pressure on crack growth in elastomers\*

G. J. Lake† and A. G. Thomas‡

Malaysian Rubber Producers' Research Association, Tun Abdul Razak Laboratory, Brickendonbury, Hertford SG13 8NL, UK

and C. C. Lawrence

Polytechnic of East London, London, UK

(Received 10 October 1991; revised 19 May 1992; accepted 2 June 1992)

The effect of immersion in a non-swelling liquid under pressure on time-dependent crack growth has been studied for various elastomers. A large effect of pressure is observed, with the rate of growth decreasing by approaching three orders of magnitude per kbar. It appears that the effect is mainly associated with the change in glass transition temperature although other factors may also be involved, such as the tendency of the failing material at the tip to separate into filaments. Measurements of strains at the crack tip suggest that this tendency may be associated with the presence of stresses through the thickness of the material.

(Keywords: hydrostatic pressure effects; elastomer; crack growth)

## INTRODUCTION

When a vulcanized elastomer which does not strain-crystallize is torn, the appearance of the surfaces of the tear in general changes with the rate of tear propagation<sup>1,2</sup>. At relatively low rates the surfaces are rough on a scale of typically a few tenths of a millimetre, but at progressively higher rates a more or less abrupt transition occurs to a smooth surface, usually accompanied by a sudden increase in rate as it is difficult to control this directly. It has been suggested that this transition may be due to suppression of a cavitation process immediately ahead of the crack tip<sup>2</sup>. Indeed, cavitation has been proposed as a mechanism for crazing in glassy plastics<sup>3</sup>.

Cavitation in elastomers is thought to be initiated from flaws which grow primarily due to a hydrostatic tensile stress, and ahead of the crack there will be not only a high stress perpendicular to the plane of the crack but also significant stress components in the other directions, which would be expected to give a substantial hydrostatic resultant. The magnitude of the hydrostatic stress required to produce cavitation can be remarkably small—generally of the order of the Young's modulus which is usually  $\sim 2$  MPa. It has in fact been found that, within limits, this modulus is often the main determining factor rather than the intrinsic strength<sup>4,5</sup>. It was suggested that the rough-smooth transition might be due to a viscoelastic increase in modulus of the elastomer ahead of the propagating tip with increasing deformation rate<sup>2</sup>, thus suppressing cavitation. It has been well established<sup>6-8</sup> that the viscoelastic behaviour of an

elastomer can have a strong influence on its strength, the greater the mechanical hysteresis the higher being the strength. Imposition of a hydrostatic pressure causes an increase in the glass transition temperature ( $\theta_G$ ) and thus an increase in hysteresis<sup>9,10</sup>. A corresponding increase in strength would therefore be expected on this account.

Non-crystallizing elastomers often show time-dependent mechanical crack growth under constant load or extension<sup>11,12</sup>. This feature is utilized in the present work to enable the effect of pressure on the crack growth behaviour to be investigated without the need for a mechanical drive to be transmitted into the high pressure chamber. Some measurements of the state of strain at a crack tip are also reported.

## EXPERIMENTAL

The high pressure experiments were conducted in an industrial autoclave located in a temperature controlled room (see *Figure 1*). The working range of the autoclave was 0–2 kbar and the chamber was 75 mm in diameter with a usable depth of 580 mm. Experiments were carried out under a liquid in order to avoid dissolution of gas into the rubber, the liquid chosen being essentially non-swelling (a commercial grade of ethylene glycol). As a check, swelling tests were carried out at high pressure. Most ethylene glycol was absorbed by the styrene-butadiene rubber (SBR) vulcanizate which showed an uptake of 1.2% after 34 days at  $\sim 1.5$  kbar.

A test piece containing a crack and held at fixed extended length by means of a suitable jig (*Figure 2c*) was placed in the chamber which was then sealed and pumped up to the required pressure. The crack length was measured initially and on removal of the jig from the chamber after a suitable period of immersion,

\* Presented at 'Physical Aspects of Polymer Science', 9–11 September 1991, University of Leeds, UK

† To whom correspondence should be addressed

‡ Consultant

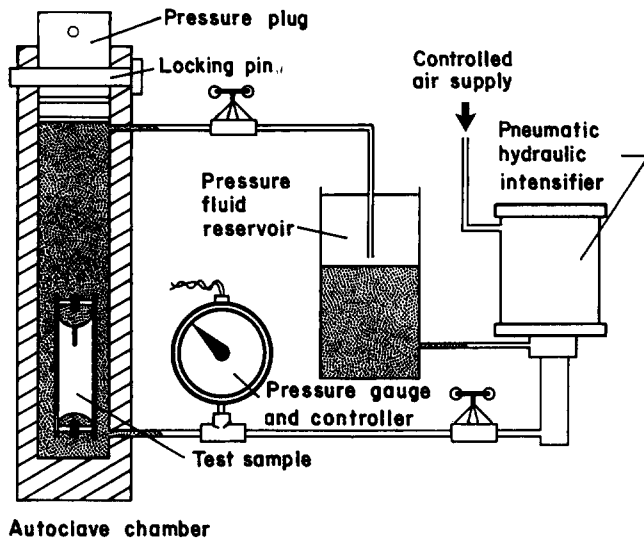


Figure 1 Schematic diagram of the high pressure system

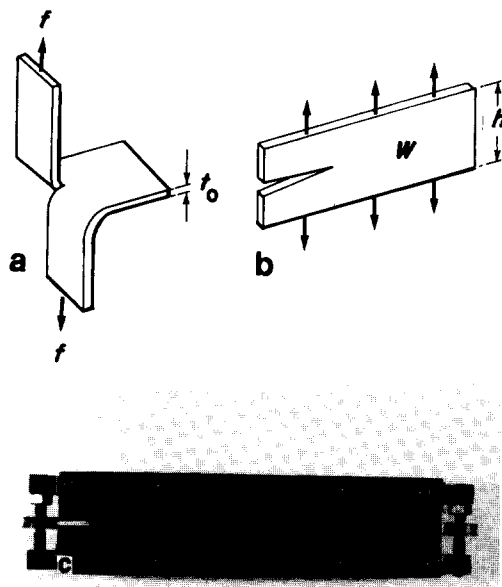


Figure 2 Test pieces used for crack growth measurements: (a) trousers test piece; (b) pure shear test piece; (c) jig used for holding a pure shear test piece at constant extension containing a test piece bonded to end plates

enabling the rate of crack growth at the high pressure to be determined. During installation and removal, the test piece spent short periods at pressures below the test pressure (mostly at atmospheric pressure). In most experiments the effect of these periods on the measured crack growth was negligible but where necessary a correction was made based on the growth rate at atmospheric pressure (which was measured in any case for reference purposes). Experiments were carried out at various deformations and pressures. The test temperature for the high pressure experiments was  $22 \pm 2^\circ\text{C}$ . Most of the control measurements (at atmospheric pressure) were also carried out at this temperature but some measurements were made at 0 or  $-20^\circ\text{C}$ .

#### Materials and test pieces

Most of the experiments were carried out with a vulcanizate of SBR but some results are also reported for an acrylonitrile-butadiene rubber (NBR) and an

ethylene-propylene rubber (EPDM). Details of mix formulations and vulcanization conditions are given in Table 1. The vulcanizates were prepared either as  $\sim 230 \text{ mm} \times \sim 230 \text{ mm} \times 2 \text{ mm}$  thick sheets from which 'trousers' test pieces (Figure 2a) or pure shear test pieces (Figure 2b) could be cut, or were moulded directly as pure shear test pieces bonded to steel end plates by means of suitable bonding agents (Figure 2c). In the latter case the test piece dimensions were  $200 \text{ mm} \times 20 \text{ mm} \times 2 \text{ mm}$  thick. Subsidiary elasticity and other measurements were also carried out on appropriate test pieces cut from the sheets.

High pressure experiments were carried out entirely with pure shear test pieces. Trousers test pieces were used additionally for control measurements at atmospheric pressure.

#### Fracture mechanics method

Various test pieces in addition to those shown in Figure 2 have been used for the evaluation of tear or crack growth behaviour of elastomers. It has been established<sup>1,12,13</sup>, with some limitations, that results from all of them are equivalent when expressed in terms of the energy available to produce crack growth, or the 'tearing' energy  $G$ . This assumption is the basis of the fracture mechanics approach. In the present work, with non strain-crystallizing elastomers, it has been convenient to use the two geometries shown in Figure 2.

For the 'trousers' test pieces (Figure 2a), provided extension of the legs is prevented (as was achieved in the present experiments by a suitable backing),  $G$  is given by<sup>13</sup>:

$$G = \frac{2f}{t_0} \quad (1)$$

where  $f$  is the force used and  $t_0$  is the test piece thickness. The lack of dependence on the modulus of the elastomer is useful because the modulus is often somewhat uncertain, due to the imperfect elasticity of the material. This test piece was therefore used to evaluate the crack growth behaviour at atmospheric pressure. Since relatively low growth rates were being studied, the method used was simply to hang a weight on the leg and measure its movement with time.

Table 1 Vulcanizate details<sup>a</sup> and glass transition temperatures of the elastomers

Vulcanizate	A	B	C
Styrene-butadiene rubber (SBR, Intol 1500)	100	—	—
Acrylonitrile-butadiene rubber (NBR, Polysar Krynac 801)	—	100	—
Ethylene-propylene rubber (EPDM, Nordel 2522)	—	—	100
Zinc oxide	3.5	3	5
Stearic acid	2.5	0.5	1
Sulphur	2	1.5	0.5
Cyclohexyl benzothiazyl sulphenamide	1.1	—	—
Dibenzothiazyl disulphide	—	1	1.5
Tetramethylthiuram disulphide	—	—	0.25
Isopropyl-phenyl paraphenylenediamine (Nonox ZA)	1	1	—
Vulcanization time (min)	60	60	60
Vulcanization temperature ( $^\circ\text{C}$ )	150	140	150
Glass transition temperature, $\theta_G$ ( $^\circ\text{C}$ ) <sup>b</sup>	-60	-22	-66

<sup>a</sup> All quantities are in parts by weight

<sup>b</sup> Determined by d.s.c., at a heating rate of  $20^\circ\text{C min}^{-1}$

For the 'pure shear' test piece shown in *Figure 2b*, the geometry chosen is with the height sufficiently small compared with the width, so that there is a region in pure shear, and with the cut sufficiently long so that there is an essentially unstrained region near that edge. With the test piece rigidly clamped or bonded along the upper and lower edges (*Figure 2c*), and extended in the direction of the arrows (*Figure 2b*),  $G$  is given by<sup>13</sup>.

$$G = Wh_0 \quad (2)$$

where  $W$  is the elastic strain energy density in the pure shear region and  $h_0$  is the unstrained value of the height,  $h$ . The value of  $W$  is calculated from the measured strain and from the pure shear stress-strain relation determined independently. As it is strictly the elastic energy released by crack growth that provides the driving force, the energy released by the elastomer on retraction is really what is relevant and this is affected by, for example, stress relaxation occurring while the test piece is held strained during crack growth. Estimates were made of this possible source of error when the experiments were interpreted but, in the context of the results, uncertainties were generally not large and allowance was made when necessary.

## RESULTS AND DISCUSSION

*Figure 3* shows the crack growth results at atmospheric pressure and room temperature (20°C) for the materials used. It can be seen that the trousers and pure shear test piece results are consistent with each other. This confirms that the experimental technique is adequate, and also gives some further assurance as to the applicability of the fracture mechanics approach. The behaviour of the

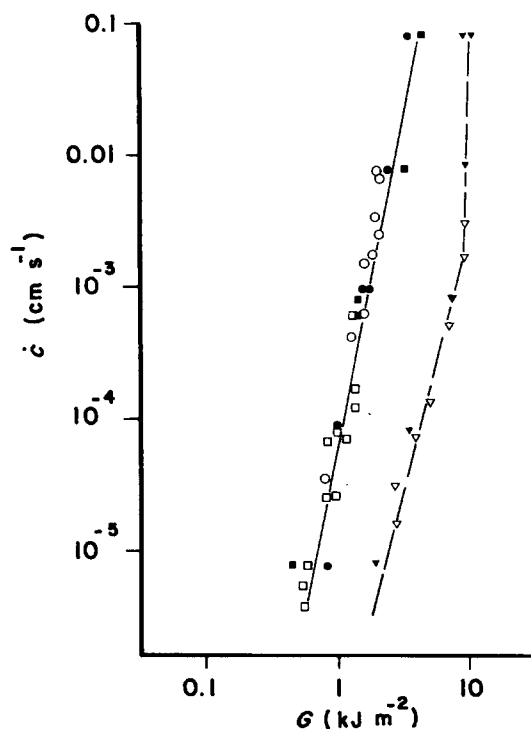


**Figure 3** Time-dependent crack growth rate  $\dot{c}$  versus strain energy release rate  $G$  (logarithmic scales) for various vulcanizates (see *Table 1*) at atmospheric pressure at  $\sim 20^\circ\text{C}$ : (○, ●) SBR vulcanizate A; (▽, ▼) NBR vulcanizate B; (□, ■) EPDM vulcanizate C; solid symbols were obtained with trousers test pieces (*Figure 2a*) and open symbols with pure shear test pieces (*Figures 2b* and *c*)

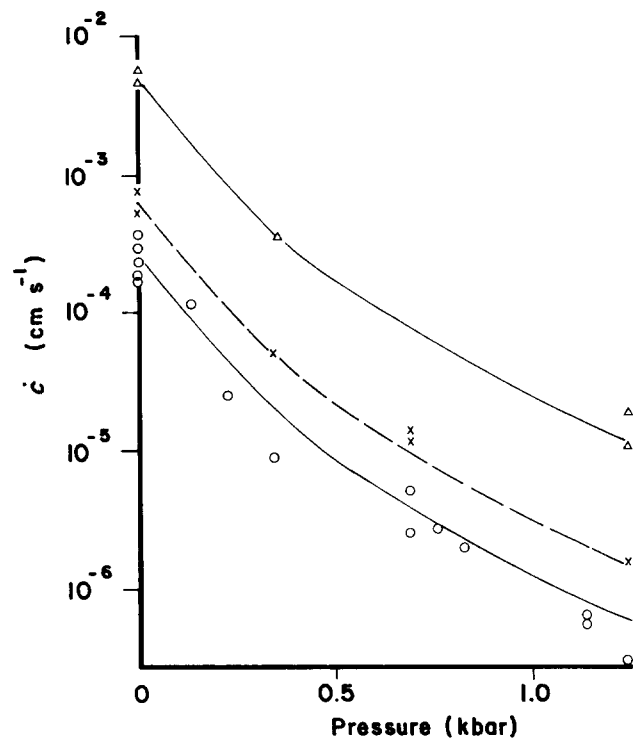


**Figure 4** Time-dependent crack growth rate  $\dot{c}$  (logarithmic scale) versus pressure for SBR vulcanizate A at  $\sim 20^\circ\text{C}$  and  $G$  values of (○) 1.0, (×) 1.4 and (△) 2.0  $\text{kJ m}^{-2}$

SBR and EPDM vulcanizates is similar but that of the NBR differs substantially. These features are broadly in accord with the relative  $\theta_G$  values of the elastomers (see *Table 1*).

Most of the work at high pressure was carried out on the SBR elastomer. This material has perhaps been the most widely studied of the non-crystallizing elastomers so that there is a large amount of published data to give background information at atmospheric pressure. There is, for example, information on the changes in surface appearance with crack growth rate<sup>2</sup>. *Figure 4* shows results for this material up to pressures of 1.3 kbar for a range of tearing energies. A strong dependence of growth rate  $\dot{c}$  on pressure is seen,  $\dot{c}$  changing by about three orders of magnitude over the range studied. Results for different  $G$  values give essentially parallel relations on this semi-logarithmic plot. *Figure 5* demonstrates this by showing  $\dot{c}$  scaled by its value at atmospheric pressure. Data at different  $G$  values are consistent with a single curve (shown by the solid line) within the accuracy of the experiments.

It is well known that the crack growth behaviour of non-crystallizing elastomers can be strongly affected by temperature and that this variation parallels that of the viscoelastic behaviour. The effect of temperature on time-dependent crack growth for the SBR vulcanizate at an approximately constant  $G$  value is shown by the data points in *Figure 6* (note, the temperature scale is reversed since an increase in pressure is equivalent to a fall in temperature). The rate of growth decreases by about three orders of magnitude over the range from +20 to  $-20^\circ\text{C}$ , this variation thus being similar to that obtained in the high pressure experiments. The interrelation between the effects of rate and temperature on the viscoelastic behaviour can be described by the well known Williams, Landel and Ferry (WLF) transform which in

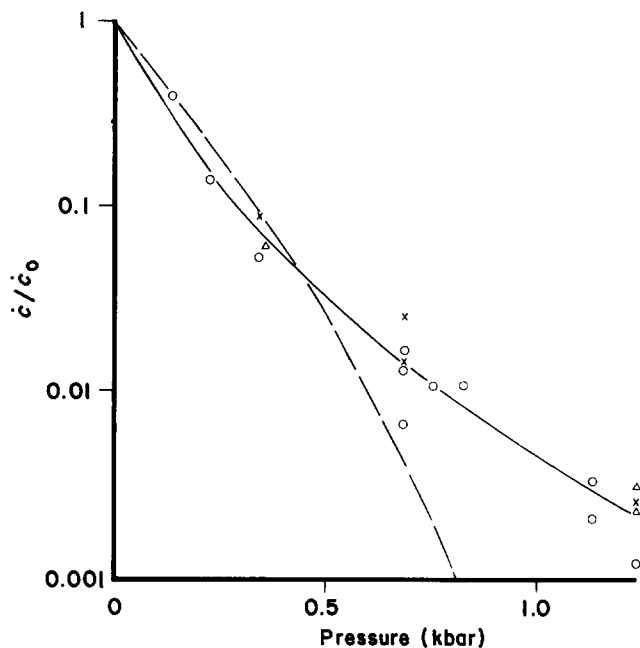


**Figure 5** Crack growth data of *Figure 4* reduced by dividing by the rate of growth at atmospheric pressure ( $\dot{c}_0$ ); the different symbols represent different  $G$  values (as in *Figure 4*). The broken line shows the form indicated by the WLF relation [equation (3)] drawn assuming 1 kbar to be equivalent to a temperature change of 52°C

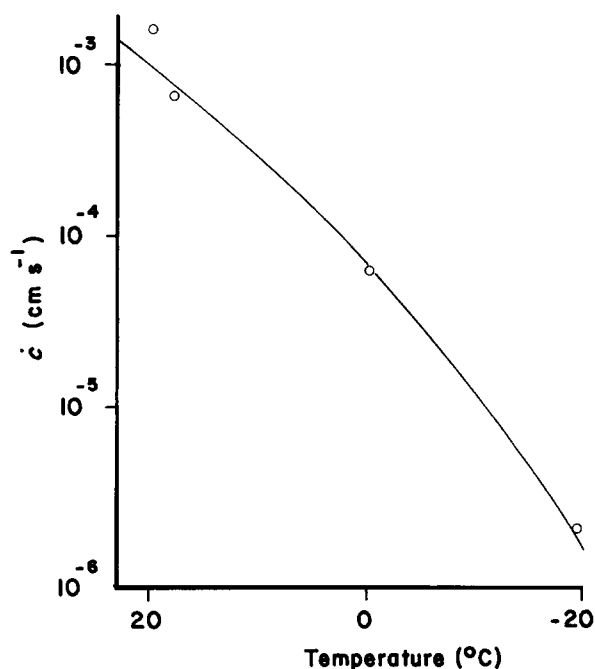


**Figure 6** Time-dependent crack growth rate  $\dot{c}$  (logarithmic scale) versus temperature (reversed scale) for SBR vulcanizate A; the line shows the dependence indicated by the WLF relation [equation (3)] with  $\theta_G$  taken as  $-60^\circ\text{C}$

its standard form is<sup>14</sup>:

$$\log \alpha_\theta = \frac{-8.86(\theta - \theta_s)}{101.6 + \theta - \theta_s} \quad (3)$$

where  $\alpha_\theta$  is the shift factor by which the rate has to be multiplied and  $\theta_s$  is a reference temperature which is taken as  $\theta_G + 50^\circ\text{C}$ . The solid line in *Figure 6* shows the relation predicted from equation (3) if  $\alpha_\theta$  is applied to  $\dot{c}$ ,

taking the  $\theta_G$  for SBR to be  $-60^\circ\text{C}$ . As can be seen, the curve fits the experimental results very well. To some extent this may be fortuitous as the present data are limited and in earlier work<sup>7,8</sup> the transform required to describe the dependence of the crack growth behaviour on temperature was found to differ somewhat from equation (3). In addition, in the present experiments the fracture surface occurring at  $-20^\circ\text{C}$  was found to be appreciably smoother than that at 0 or  $+20^\circ\text{C}$  (*Figure 7*). Thus if there had been no change in the fracture surface roughness (and hence crack tip diameter), the rate of growth at  $-20^\circ\text{C}$  would have been lower still.

A curve derived from that in *Figure 6* is also shown (as the broken line) with the high pressure results in *Figure 5*, the curve being fitted at the lower end by choosing a temperature–pressure equivalence of 52°C per kbar. As can be seen, this curve is of the wrong shape to describe the pressure dependence of the crack growth rate. Furthermore, the required pressure–temperature equivalence is about twice that previously estimated from mechanical measurements for elastomers<sup>9,10</sup>. Thus it appears that the effect of hydrostatic pressure on crack growth does not simply arise from the associated change in  $\theta_G$ . If the temperature–pressure equivalence of some 25°C per kbar given in the literature is assumed, then at the lower end of the pressure range covered the effect of pressure is greater than expected from the change in  $\theta_G$ , while at the higher end it is less, perhaps because the free volume available is diminishing more rapidly. *Figure 8* shows fracture surfaces (for the same  $G$  value) at different pressures and it is apparent that there is much less change in appearance than when the temperature is varied. Thus there is no evidence, from these experiments, that the hydrostatic pressure produces any appreciable change in fracture surface roughness, as might have been expected if cavitation were being suppressed.

High pressure experiments with the EPDM and NBR are at an early stage. Nevertheless, the initial results, which are shown in *Figure 9*, indicate similar effects of pressure to that observed with SBR. In these results, the rate of growth is slightly higher for the NBR but it may be noted that the energy level is considerably higher, consistent with the crack growth characteristics of *Figure 3*.

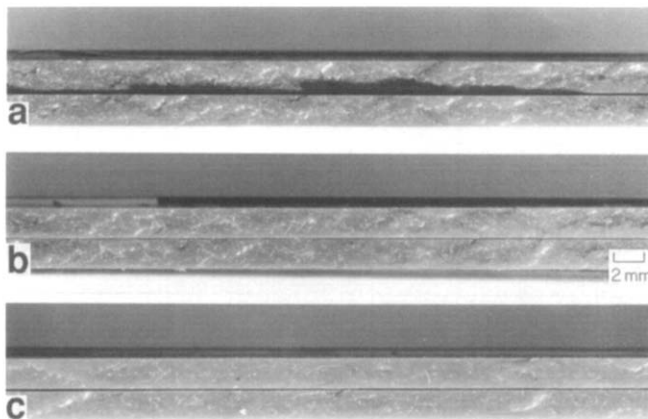


**Figure 7** Effect of test temperature on fracture surface appearance for SBR vulcanizate A at atmospheric pressure and with  $G = 1.6 \text{ kJ m}^{-2}$  throughout at: (a)  $+20^\circ\text{C}$ ; (b)  $0^\circ\text{C}$ ; (c)  $-20^\circ\text{C}$ ; both fracture surfaces (approximately aligned) are shown in each case

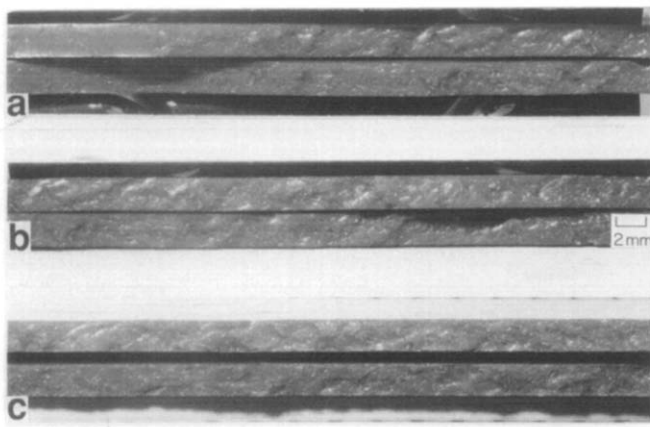


**Figure 8** Fracture surface appearances for various test pressures for SBR vulcanizate A at  $\sim 20^\circ\text{C}$  and with  $G = 1.9 \text{ kJ m}^{-2}$  throughout at: (a) 1 bar; (b) 360 bar; (c) 1240 bar

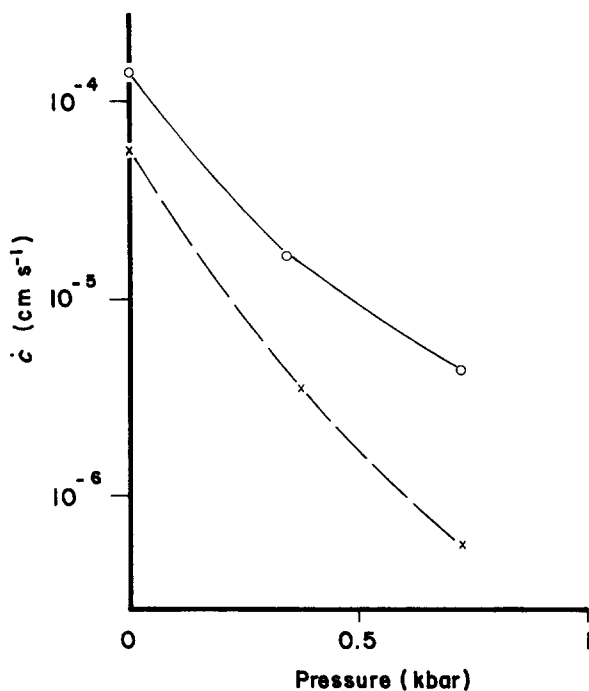


**Figure 9** Time-dependent crack growth rate  $\dot{c}$  (logarithmic scale) versus pressure for (○) NBR vulcanizate B with  $G = 4.3 \text{ kJ m}^{-2}$  and (×) EPDM vulcanizate C with  $G = 0.8 \text{ kJ m}^{-2}$

#### State of strain at the crack tip

The state of strain at the crack tip is clearly of interest in relation to cavitation and other possible effects in fracture. Visual observation on a test piece of natural rubber (which is convenient to use as, under the conditions employed, this material exhibits little or no time-dependent growth) shows that the thickness at the tip is often appreciably greater than would be expected if the material there were in simple extension at its breaking extension ratio  $\lambda_b$  (typically approaching 9 for natural rubber). Thus the rubber at the tip seems to be stressed perpendicular to the plane of the sheet. The breaking elongation  $\lambda_b$  is, however, not likely to be significantly affected by these stresses since even in equi-biaxial tension (as in bursting a balloon<sup>15</sup>) the breaking elongation is much the same as in simple tensile failure. The normal stresses presumably arise because the effective radius of the crack tip is substantially less than

the sheet thickness. There is evidence<sup>16</sup> that the  $G$  value is related to the work to break per unit volume  $W_b$  of the material at the tip and the tip diameter  $d$  by:

$$G = dW_b$$

giving

$$d = \frac{G}{W_b} \quad (4)$$

From dimensional considerations, it can be deduced that the strained thickness  $t$  at the tip is related to  $d$  and  $t_0$  by:

$$t/t_0 = \lambda_2 = f(d/t_0, \lambda_b) \quad (5)$$

where  $f$  represents an unknown function and assuming that  $W_b$  (like  $\lambda_b$ ) is not much affected by the stresses perpendicular to the plane of the test piece. Thus with equation (4) we have

$$\lambda_2 = f(G/t_0, \lambda_b) \quad (6)$$

Figure 10 shows some results obtained with a natural rubber vulcanizate for various sheet thicknesses  $t_0$  employing a trousers test piece. The figure shows that results for the various thicknesses superimpose satisfactorily on a single curve in accordance with equation (6), giving support to the above interpretation. The broken horizontal line indicates the  $\lambda_2$  value expected assuming no stress occurs perpendicular to the plane of the test piece, i.e. with the tip in simple extension, and shows the substantial magnitude of the departures.

To enable  $\lambda_2$  to be determined dynamically, preliminary measurements have been made with a video camera focused on the crack tip (looking in the thickness direction) as a crack grows in a time-dependent manner. Figure 10 also shows results obtained in this way for the EPDM rubber. They are qualitatively similar to the natural rubber results but would not be expected to be identical as the  $\lambda_b$  values are likely to be different.

Thus, under many circumstances there will be appreci-

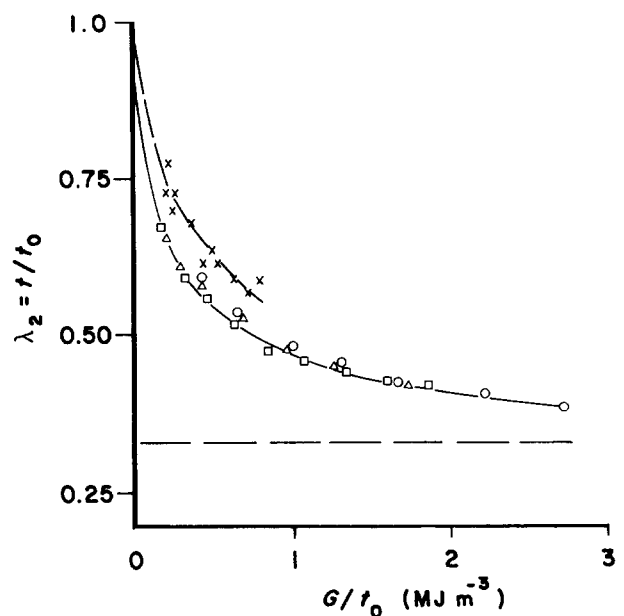


**Figure 10** Extension ratio at the crack tip in the thickness direction  $\lambda_2$  versus ratio of strain energy release rate ( $G$ ) to the unstrained thickness ( $t_0$ ). For a natural rubber vulcanizate  $t_0$  is (○) 1.6, (△) 2.6 and (□) 3.5 mm. For EPDM vulcanizate C,  $t_0$  is (×) 2.05 mm; the broken line shows an example of a relationship that would apply if the tip were in simple extension

able stress, of a tensile nature, in the thickness direction at a crack tip, arising from geometrical sources. Whether this is sufficient, in itself, to cause cavitation is uncertain at present. However, it appears that the tendency of the failing material to form filaments, which is often observed, may be directly associated with this stress component.

## CONCLUSIONS

The work shows that hydrostatic pressure has a large effect on time-dependent crack growth in elastomers, the rate of growth decreasing by some three orders of magnitude when the pressure is increased to  $\sim 1.3$  kbar. The relative effect of pressure on the rate appears to be similar for elastomers with differing  $\theta_G$  values and for various energy release rates within the range covered. The effect of pressure does not seem to be associated solely with the corresponding change in the  $\theta_G$ , although this appears almost certain to be a major contributory factor.

The results obtained so far provide no evidence that cavitation plays a part in the crack growth process, but they are not sufficiently extensive for this possibility to

be ruled out. It appears that transverse stresses will often be present at the crack tip and may be responsible for the separation of the failing material into filaments with cavities in between them.

## REFERENCES

- 1 Thomas, A. G. *J. Appl. Polym. Sci.* 1960, **3**, 168
- 2 Kadir, A. and Thomas, A. G. *Rubber Chem. Technol.* 1981, **54**, 15
- 3 Gent, A. N. *J. Mater. Sci.* 1970, **5**, 925
- 4 Gent, A. N. and Lindley, P. B. *Proc. R. Soc. A* 1958, **249**, 195
- 5 Gent, A. N. and Denecour, R. L. *J. Polym. Sci. A2* 1968, **6**, 1853
- 6 Smith, T. L. *J. Polym. Sci.* 1958, **32**, 99
- 7 Mullins, L. *Trans. Inst. Rubb. Ind.* 1959, **35**, 213
- 8 Gent, A. N. and Henry, A. W. 'Proc. Int. Rubb. Conf.', Maclaren, London, 1967, p. 193
- 9 Singh, H. and Nolle, A. W. *J. Appl. Phys.* 1959, **30**, 337
- 10 McKinney, J. E., Belcher, H. V. and Marvin, R. S. *Trans. Soc. Rheol.* 1960, **IV**, 347
- 11 Greensmith, H. W. and Thomas, A. G. *J. Polym. Sci.* 1955, **18**, 189
- 12 Lake, G. J. and Lindley, P. B. *J. Appl. Polym. Sci.* 1964, **8**, 707
- 13 Rivlin, R. S. and Thomas, A. G. *J. Polym. Sci.* 1953, **10**, 291
- 14 Williams, M. L., Landel, R. F. and Ferry, J. D. *J. Am. Chem. Soc.* 1955, **77**, 3701
- 15 Stevenson, A. and Thomas, A. G. *J. Phys. D* 1979, **12**, 2101
- 16 Thomas, A. G. *J. Polym. Sci.* 1955, **18**, 177